Research Article **AJSRE (2018), x:xx**

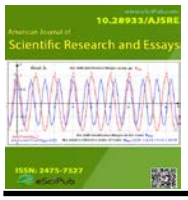

American Journal of Scientific Research and Essays (ISSN:2475-7527)

Implementation of IFOC Algorithm for a Three-Phase Induction Motor Embedded on DSP Microcontroller

Denis Carlini Alexandre, Alexandre Simiao Caporali and Cesar da Costa

IFSP Institute Federal of São Paulo, São Paulo, Brasil.

ABSTRACT

Asynchronous machines are well known to have natural limitations because of the highly nonlinearity and complexity of their motor models. To resolve these problems, an indirect field-oriented control (IFOC) algorithm is applied to control the instantaneous electrical quantities such as torque and flux component. Medium-voltage drives are generally based on either voltage-source inverter (VSI) or current-source inverter (CSI). This paper presents a high-performance CSI-fed IFOC method. By the decoupled control of the machine flux and torque, the performance of the conventional direct field-oriented control (DFOC) CSI-fed induction motor drives has improved; however, this scheme presents a low dynamic response and machine parameter dependence. A squirrel-cage induction motor drive system that provides the proposed IFOC algorithm is tested. The IFOC algorithm has a good dynamic performance and stability. Graphs with measured and estimated values of torque and speed are presented. The results demonstrate the efficiency of the proposed torque control embedded on a digital signal processor (DSP) microcontroller.

Keywords: IFOC algorithm, Embedded system, Three-phase induction motor, Torque control

***Correspondence to Author:**
Cesar da Costa
IFSP Institute Federal of São Paulo, São Paulo, Brasil.

How to cite this article:
Denis Carlini Alexandre, Alexandre Simiao Caporali and Cesar da Costa. Implementation of IFOC Algorithm for a Three-Phase Induction Motor Embedded on DSP Microcontroller. American Journal of Scientific Research and Essays, 2018 x:xx.

eSciPub LLC, Houston, TX USA.
Website: http://escipub.com/

INTRODUCTION

Three-phase induction motors are the most widely used motors in industrial motion control systems because of their reliability, robustness, and simplicity of control. Until a few years ago the AC motor could either be plugged directly into the mains supply or controlled by the well-known scalar V/f method. However, many applications require variable speed operation. The scalar V/f method can provide speed variation but does not handle transient condition control and is valid only during a steady state. This method is most suitable for applications without position control requirements or the need for high accuracy of speed control, and it leads to over-currents and over-heating, which necessitate a drive; therefore, the method becomes cluttered and is no longer cost-effective. Examples of these applications include heating, air conditioning, fans and blowers (Novotny et al., 2000; Leonard, 2001).

In the last two decades, the study of speed and torque control in three-phase induction motors has gained much attention. Most researchers have focused on field-oriented control (FOC) strategies based on current-source inverter (Guo et al., 2017; Martinez-Hernandez et al., 2016). The FOC offers a solution to circumvent the need to solve high-order equations with many variables and nonlinearities and achieve an efficient control with high dynamics.

During the last few years, the field of electrical drives has broadened rapidly mainly because of the advantages of semiconductors in both power and signal electronics and in powerful microcontrollers and digital signal processors (DSPs). These technological improvements have allowed the development of a very effective AC drive control with lower power dissipation hardware and increasingly accurate control structures.

Casadei et al. (2013) compared the direct torque control and direct FOC (DFOC) techniques, emphasizing their advantages and disadvantages. Leedy (2013) presented a dynamic model of engines developed in MATLAB/Simulink®. This model can be employed in the study of the dynamic behavior of the induction motor and can be modified to study other topologies of motors and drives. Horváth and Kuslits (2017) presented an observer with a Kalman filter to implement the IFOC technique without the need for a rotation sensor.

Holzmüller et al. (2017) presented a method to decrease the response time of the FOC strategy. In the practical implementation of the FOC technique with a DSP, the sources of delay are in the sampling of the analog– digital converter. The response time was improved by compensating delays in the control mesh using Smith's predictive controller. The method presented was verified through simulations in MATLAB/Simulink.

This study presents a digital controller with an indirect field-oriented control (IFOC) algorithm applied to a three-phase induction motor embedded on a digital signal microprocessor. A rotor flux observer is presented, and the indirect oriented control system is implemented.

This paper is organized as follows. Section 2 provides a brief description of the three-phase induction motor. Section 3 presents a summary of vector control of the AC induction motor. Section 4 provides a description of the modeling of the indirect vector control algorithm proposed. Section 5 describes the experimental procedure. Section 6 presents the proposed indirect vector control. Section 7 provides the concluding remarks.

THREE-PHASE INDUCTION MOTOR

The AC induction motor is a rotating electrical machine designed to operate from a three-phase alternating voltage source. Asynchronous motors are based on induction. The cheapest and most widely used is the squirrel-cage motor, in which aluminum conductors or bars are cast into slots in the outer periphery of the rotor. These conductors or bars are shorted together at both ends of the rotor by cast aluminum end

rings. For variable speed drives, the source is normally an inverter that uses power switches to produce approximately sinusoidal voltages and currents controllable in terms of frequency and magnitude (Novotny et al., 2000; Leonard, 2001).

Because of the capability of such modern microcontrollers, it is possible to implement sophisticated current-source inverter based on vector control. Vector control refers not only to the magnitude but also to the phase of variables. Matrix and vectors are used to represent the control quantities. This method considers not only successive steady-states but real mathematical equations that describe the motor itself, so that the obtained results have a better dynamics for torque variations in a wider speed range (Ibrahim et al., 2015).

VECTOR CONTROL OF AC INDUCTION MOTOR

Field-oriented control involves controlling the components of the motor stator currents, represented by a vector, in a rotating reference frame with a d-q coordinate system. In a special reference frame, the expression for the electromagnetic torque of the smooth-air-gap machine is similar to the expression for the torque of the separately excited DC machine. In the case of induction machines, the control is normally performed in a reference frame aligned to the rotor flux space vector. To perform the alignment on a reference frame revolving with the rotor flux, information on the modulus and the space angle (position) of the rotor flux space vector is required. Two different strategies can be used to estimate the rotor flux vector:

●Direct Field-Oriented Control: Rotor flux vector is either measured using a flux sensor mounted in the air-gap or using the voltage equations, starting from the electrical machine parameters.

●Indirect Field-Oriented Control: Rotor flux vector is estimated using the field-oriented control equations (current model) and rotor speed measurement.

With these algorithms, the stator currents of the induction machine are separated into flux- and torque-producing components by a transformation to a d-q coordinate system.

On this reference frame, the torque component is on the q-axis and the flux component is on the d-axis. The vector control system requires the dynamic model equations of the induction motor and returns to the instantaneous currents and voltages to calculate and control the variables. The IFOC technique is described in this work.

To get the DC machine performance, the Clarke and Park transformations are needed (Guo et al., 2017). Clarke transformation is the change from a three-phase ABC reference frame to a two-phase stationary (α, β) reference frame (Fig. 1a), while park transformation is the change from a two-phase (α, β) reference frame to a rotating (d, q) reference frame (Fig. 2b). The Clarke and Park transformations are mainly used in vector control architectures related to permanent magnet synchronous machines and asynchronous machines, respectively (Sandre-Hernandez et al., 2016).

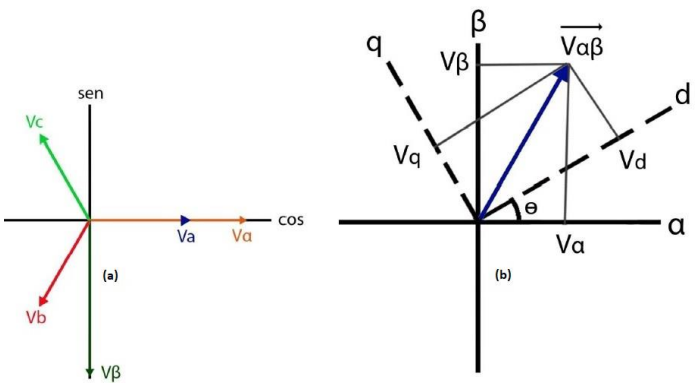

Figure 1. (a) Stationary frame A-B-C to (α, β) transformation; (b) (α, β) axes to synchronously rotating frame d-q axes transformation.

MODELING OF THE INDIRECT VECTOR CONTROL ALGORITHM

Figure 2 presents the basic scheme of torque control with the proposed IFOC algorithm.

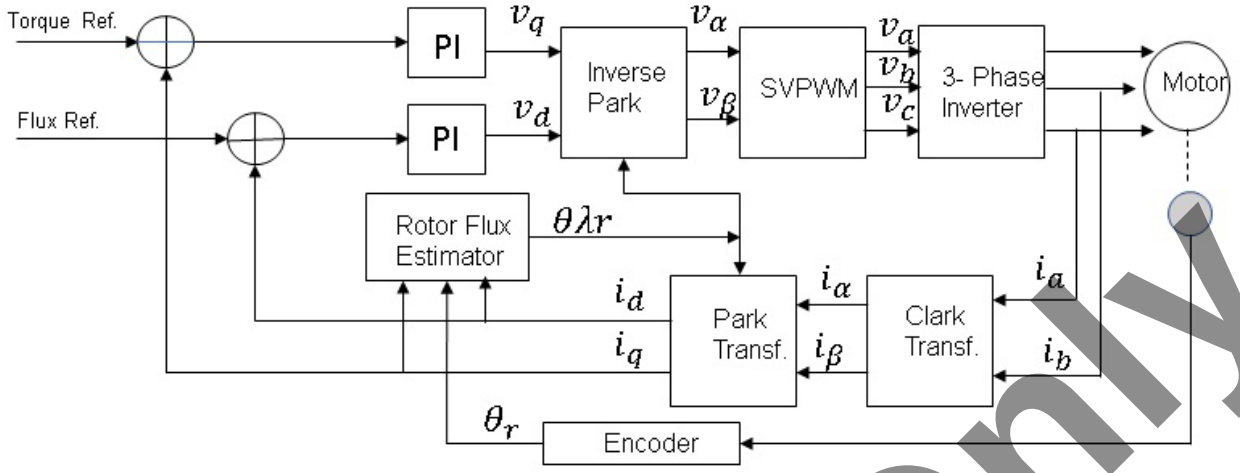

Figure 2. Schematic diagram of IFOC algorithm

Two-phase currents are fed into Clarke and Park transformation modules. The projection outputs of the Clark block are indicated with $i_{s\alpha}$ and $i_{s\beta}$. These two current components provide the input of the Park transformation that gives the current in the *d, q* rotating reference frame aligned with the rotor flux vector. The exact rotor flux angular position $\theta\lambda r$ is necessary to calculate the two components $i_{d\sigma}$ and i_{qs}. The i_{ds} and i_{qs} components are compared to i_{dref} (the flux reference) and i_{qref} (the torque reference). The torque command i_{qref} is the output of the speed regulator. The flux command i_{dref} indicates the right rotor flux command for every speed reference within the nominal value. The current regulator outputs are v_{dref} and v_{qref}. They are processed into the inverse Park transformation, and the outputs are $v_{\alpha ref}$ and $v_{\beta ref}$, which are the components of the stator vector voltage in the α, β orthogonal reference frame. These are the inputs of the space vector pulse-width modulation (PWM). The outputs of this block are the gate signals that drive the inverter. The main block of the vector control is the *current model* block. This block needs the rotor resistance and rotor inductance parameters, and the accuracy of these parameters greatly affects the performance of the control.

In Fig. 2, components i_d and i_q are the d-axis and q-axis of the rotor currents, respectively, and vd and vq are the d-axis and q-axis components of the stator voltage, respectively. Equations 1, 2, 3, and 4 show the voltage equations of the induction motor in d-q coordinate for obtaining the DC machine performance (Guo et al., 2017).

$$v_d = R_s i_d + p\lambda_d - w_s\lambda_q \quad (1)$$

$$v_q = R_s i_q + p\lambda_q - w_s\lambda_d \quad (2)$$

$$0 = R_r i_d + p\lambda_d - (w_s - w_r)\lambda_q \quad (3)$$

$$0 = R_r i_q + p\lambda_q - (w_s - w_r)\lambda_d \quad (4)$$

Here,

R_r - rotor resistance;

R_s - stator resistance;

λ_d - d-axis component of stator flux; □q - q-axis component of stator flux; ws - stator angular frequency;

w_r - rotor angular frequency;

p - differential operator.

According to Novotny et al. (2000), the torque equation in d-q coordinate is given by Eq. 5.

$$T_e = n_p \frac{L_m}{L_r}(\lambda_{dr} i_{qs}) \quad (5)$$

Here,

n_p - induction motor's pole-pair;

L_m, L_r - parameter of induction motor.

The electromagnetic torque is proportional to the product of rotor flux linkage and the stator q-axis current. This resembles the torque expression of the DC motor, which is proportional to the product of the field flux linkages and the armature current. If the rotor flux linkage is kept constant, the torque is proportional to the torque-producing component of the stator current (Guo et al., 2017). The Clarke and Park transformations are used to obtain the rotor flux λ_{dr} and the stator q-axis current i_{qs} .

EXPERIMENTAL PROCEDURE

The experimental tests were conducted using the following equipment: (1) three-phase induction motor EMsynergy®, model 800006, squirrel cage, power 0.0184 hp (13.6 W), torque 0.116 Nm, 4 poles, 14.7 V, 1121 rpm, (2) rotary and incremental encoder Omron®, model E6A2-CW5C, 200 pulses per revolution, (3) data acquisition board, National Instruments®, model NI USB-6216, (4) DSP control board, Texas Instruments®, model LaunchXL-F28027F, (5) motor drive BoostXL-DRV8301,Texas Instruments, (6) three-phase induction motor (0.5 cv, 4 poles, 1680 rpm) as load, (7) power supply, (8) PC running the application software. Figure 3 shows the experimental setup.

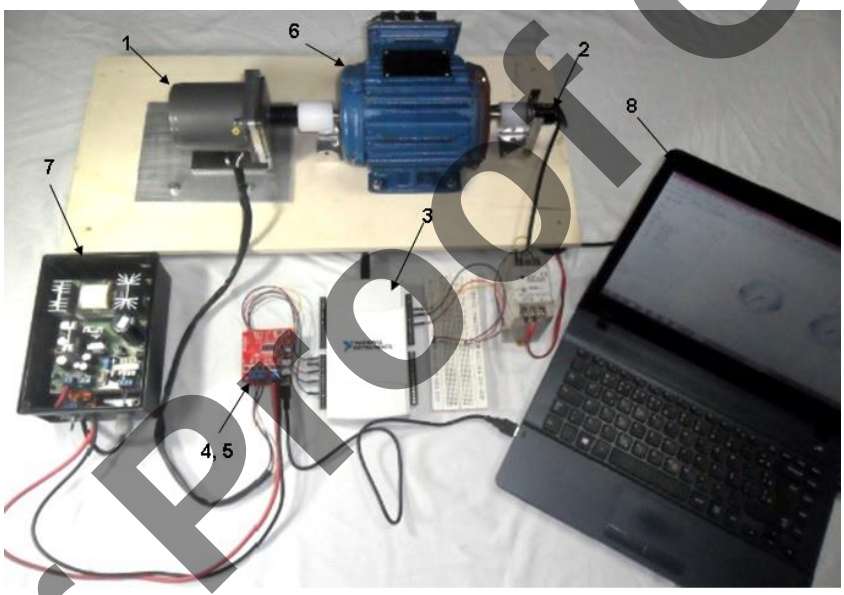

Figure 3. Experimental setup.

The LaunchXL-F28027F control board from Texas Instruments was used to demonstrate the capabilities of the TMS320F28027F microcontroller and to provide a hardware tool that allows the IFOC algorithm to be embedded.

TMS320F28027F is a 16-bit microcontroller unit with a multiplier/accumulator unit (DSP features), 32 Kbytes of flash memory, and 6 Kbytes of RAM. Its main characteristics are 60 MHz CPU, 16.67 ns instruction cycle, multiplier/accumulator unit with eight 40-bit accumulator PWM channels, seven 12-bit A/D converter channels (3 µs conversion time), and capture/compare peripherals with 32-bit timer (100 ns of maximum resolution). The BoostXL-DRV8301 board from Texas Instruments was used for the three-phase voltage power stage. The current sensing board was designed to sense the line currents. Only two-phase currents in this application were detected.

In this study, torque and rotation were estimated. The IFOC algorithm was implemented and tested, depending only on the knowledge of the induction motor parameters and the sensors that

measure the voltages and currents of the power supply. Table 1 shows the parameters of the three-phase induction motor.

Table1. Parameters of the three-phase induction motor

Parameter	Value	Parameter	Value
$R_s(\Omega)$	1.8242	$J(Kg.m^2)$	0.0766
$R_r(\Omega)$	1.2314	$L_m(H)$	0.030
$L_s(H)$	0.00545	$f(Hz)$	50
$L_r(H)$	0.00545	n_p	2

THE PROPOSED INDIRECT VECTOR CONTROL ALGORITHM

The block diagram of the IFOC algorithm embedded in the DSP microcontroller is shown in Fig. 4. The different stages of the algorithm proposed of indirect vector control are discussed here.

1) Two out of the three-phase stator currents are measured by means of the current sensors. These measurements provide i_a , i_b , while i_c is computed as

$i\chi = -i\alpha - i\beta$.

2) The three-phase currents are converted into a two-axis time-variant system. This conversion provides the variables $i\alpha$ and $i\beta$ starting from i_a , i_b , and i_c (Clark Transformation). This transformation allows the number of variables to be reduced in the voltage equations of the electrical machinery. In particular, all mutual-inductances in the stator windings are neglected.

3) The two-axis time-variant coordinate system ($i\alpha$, $i\beta$) is projected in a time-invariant rotating frame aligned with the rotor flux. The knowledge of the rotor flux angle is necessary to execute this transformation, which provides the i_d and i_q components. For steady state conditions, id and iq are constant.

4) Error signals are computed starting from the reconstructed values of i_d and i_q and their reference values. The i_d reference controls rotor flux, while the iq reference controls the torque output of the motor. The error signals constitute the input of the PI controllers which provide v_d and v_q as outputs, which are the voltage vectors to be applied to the motor.

5) The rotor mechanical position, rotor electrical time constant, and i_d and i_q are the inputs for the current model block that estimates the new rotor flux position.

6) The v_d and v_q values are rotated back to the stator reference frame using only the calculated rotor flux position. This calculation provides quadrature voltage values, v_α and v_β.

7) The v_α and v_β values are transformed back to three-phase values, *Vref1, Vref2,* and *Vref3*, constituting the voltage reference for the space vector PWM block, which can be used in calculating the new PWM duty cycle values to be applied to the motor.

RESULTS AND DISCUSSION

This experiment was performed to verify the response of the IFOC control to changes in the speed reference and load. Variations up to 1000 rpm were made considering 200 rpm as the operating point. Figure 5 shows the result of IFOC control response tests on measured and estimated speed changes.

The speed response of the motor without load reached the reference (Fig. 5). Figure 6 shows that the speed of the motor with load also responded well to the variations that were made (reference speed). The value estimated by the controller was very close to the value measured in the motor.

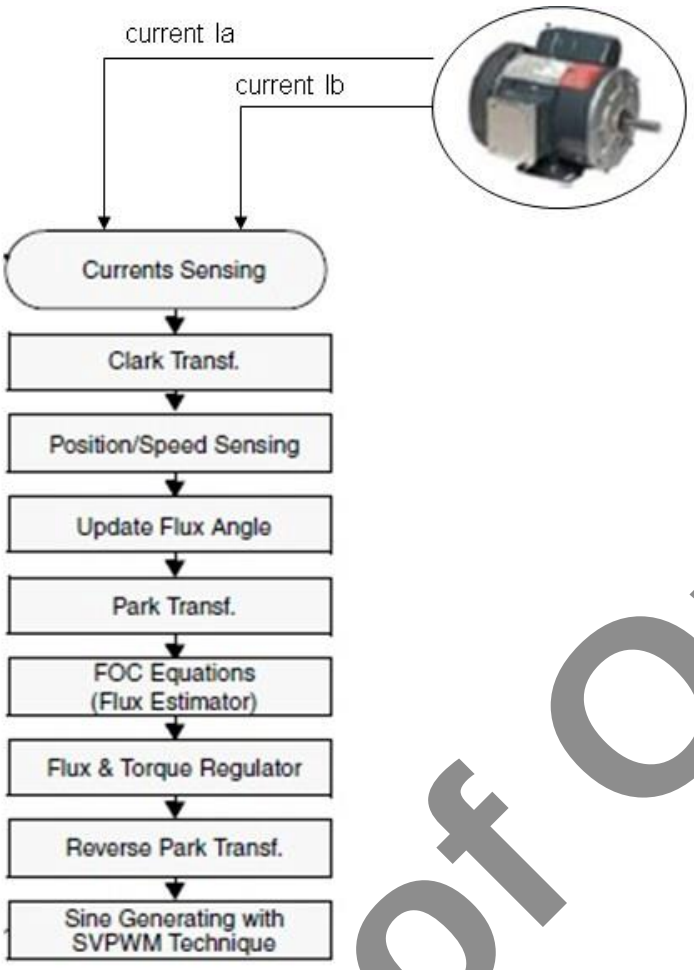

Figure 4. Block diagram of IFOC algorithm proposed.

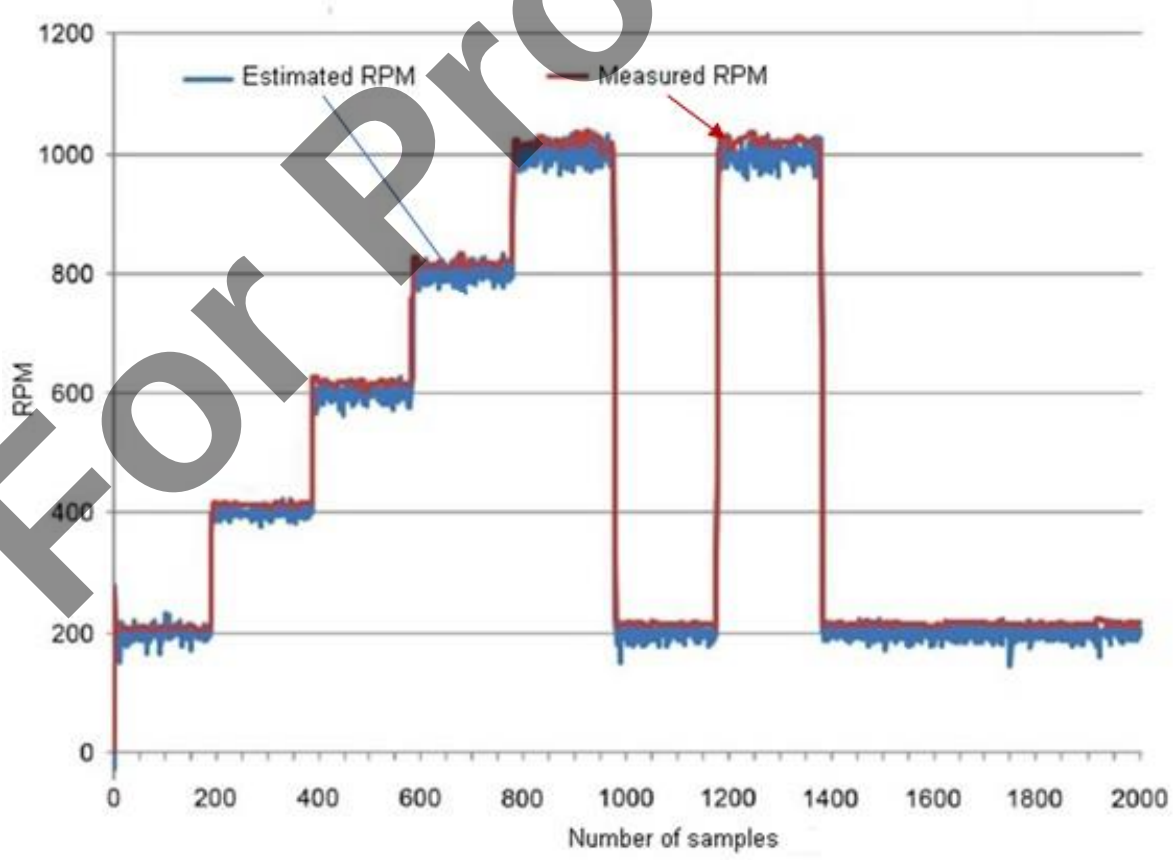

Figure 5. Results of the estimated and measured speed changes with load.

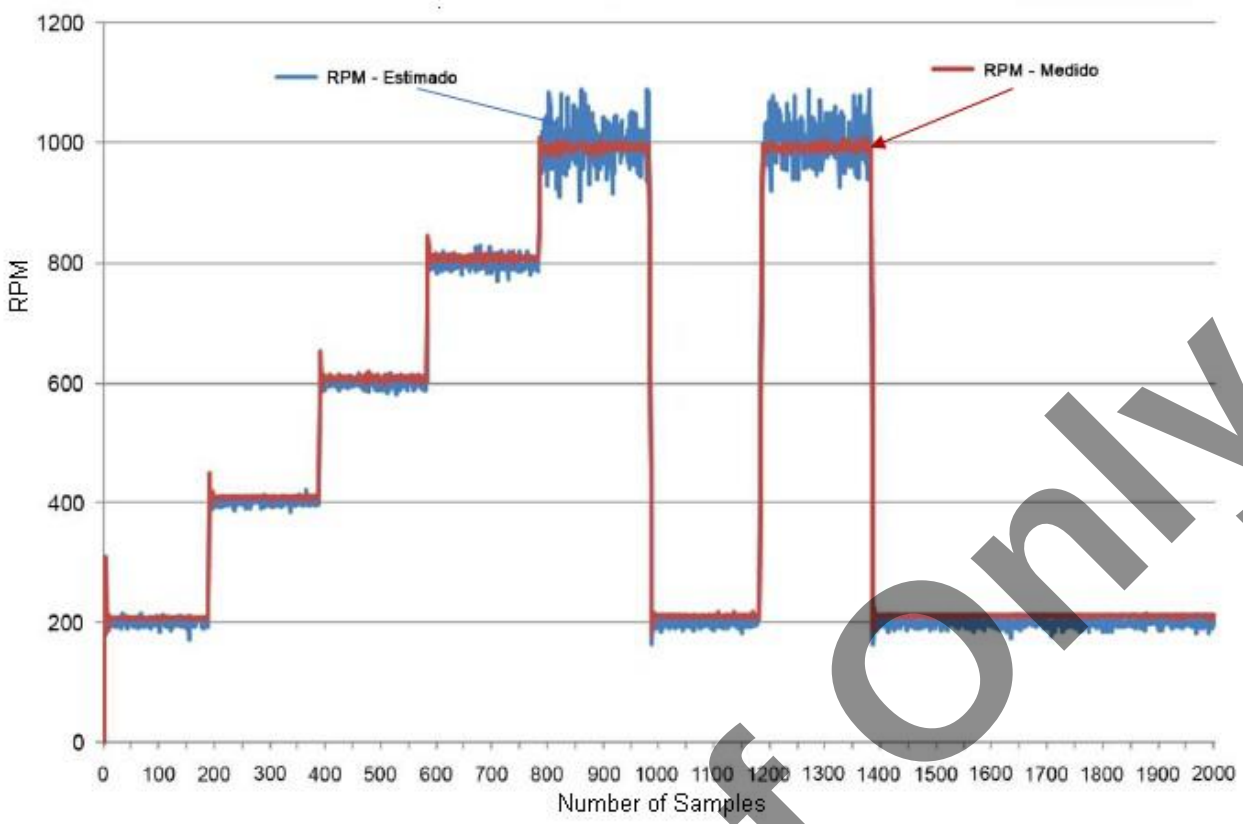

Figure 6. Results of the estimated and measured speed changes without load

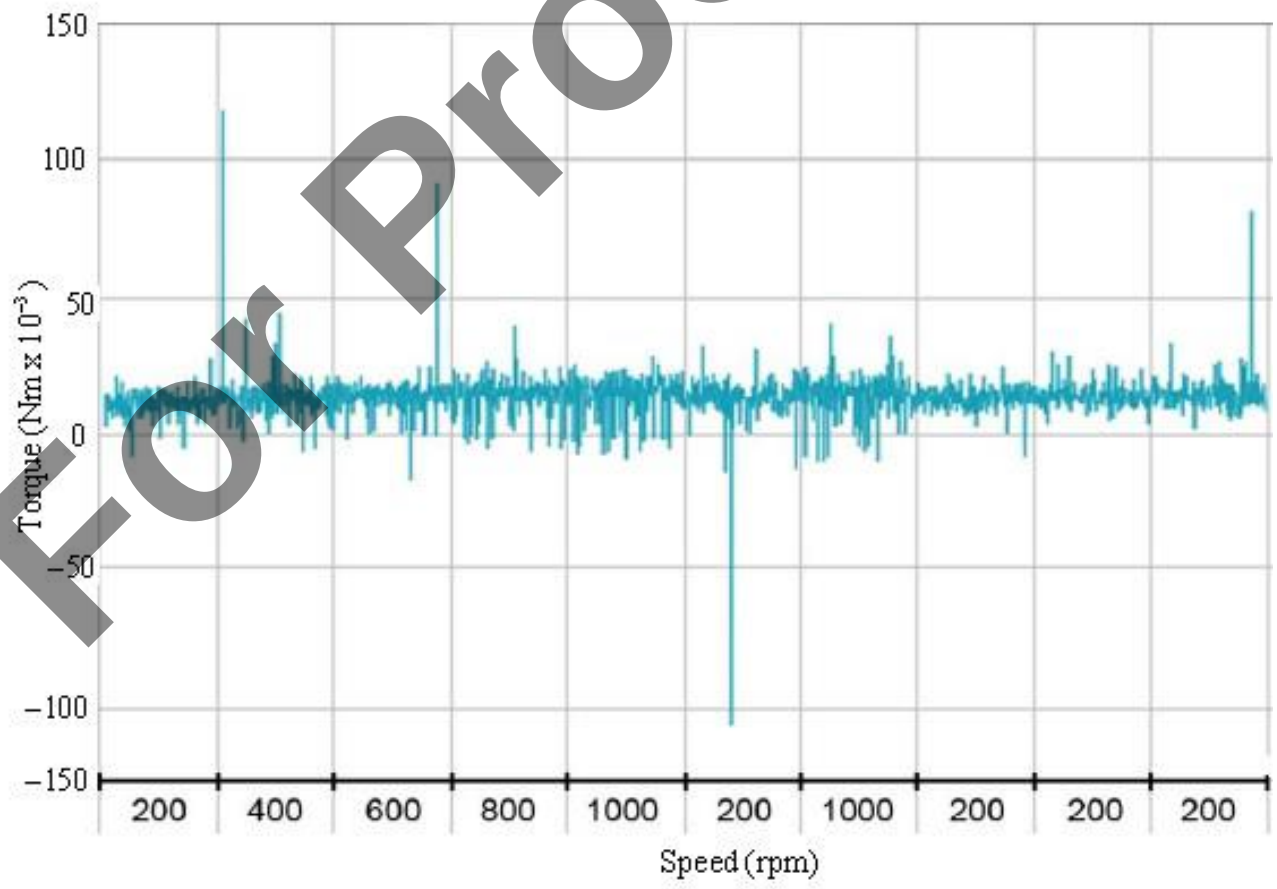

Figure 7. Graph of torque estimated by the system without load.

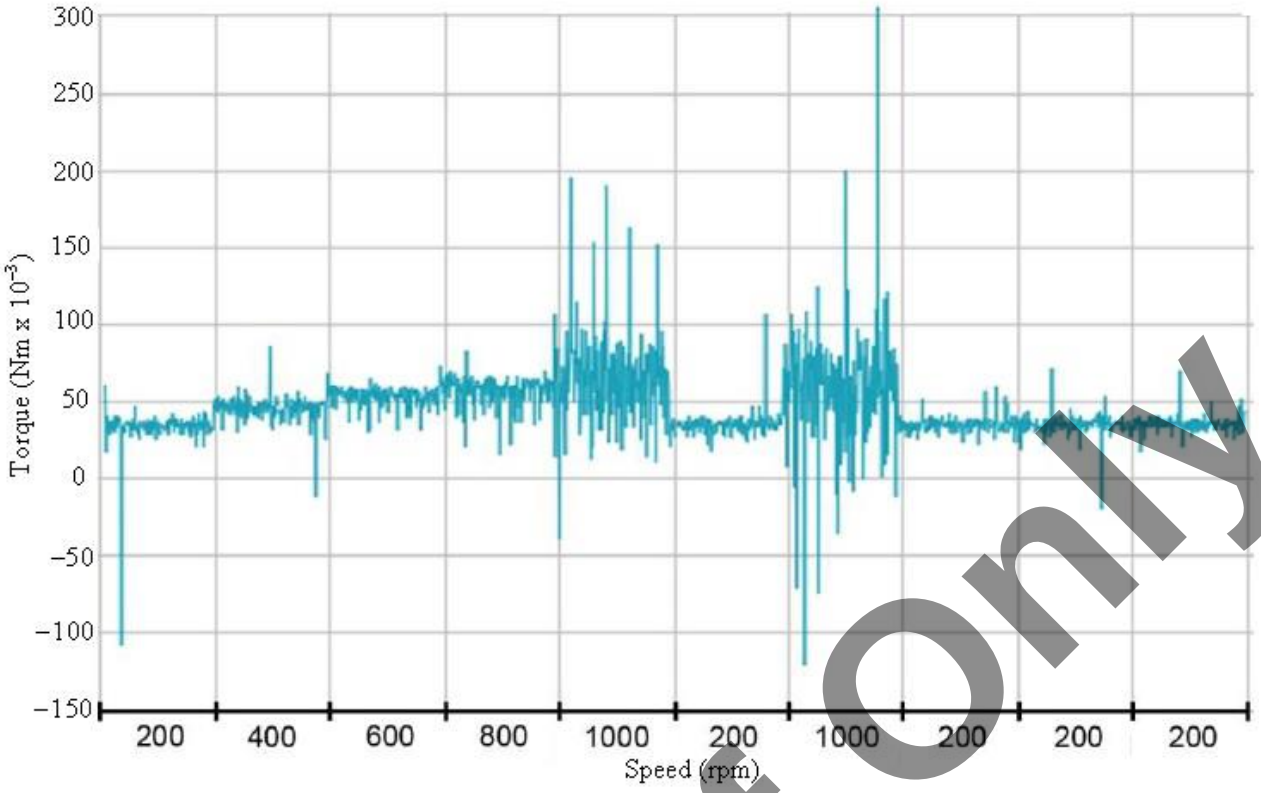

Figure 8. Graph of torque estimated by the system with load.

Figure 7 shows the behavior of the torque at different speed levels without load, and Fig. 8 shows the torque response of the motor with load.

The torque varied (Figs. 7 and 8) because the rotation of the motor shaft was the controlled quantity. The control system freely varied the torque to keep the rotation as close as possible to the reference value (set point). The instant the rotation falls below the reference value, the system increases the torque to increase the rotation. The instant the rotation is above the reference value, the system decreases the torque to decrease the rotation. The torque peaks were as a result of the Kp (proportional gain) and Ki (integral gain) variables of the proportional–integral controller. By increasing the Ki value, the control system became susceptible to oscillations; that is, the rotation of the motor shaft could oscillate. The Ki value is analogous to the spring elastic constant (Hooke's Law). By increasing the Kp value, the damping of the system was increased; that is, while Ki is analogous to the properties of a spring, Kp is analogous to the properties of a damper. The Kp and Ki values

should be used so that the system does not oscillate (undermined) or have response delays (super-dense). A sub-damped system becomes unstable when it oscillates. An over-stepping system causes delays in response. The IFOC control responded well to the variations that were made (load and reference speed).

CONCLUSION

This paper presents a vector control IFOC algorithm for three-phase induction motors. The operating principle of the IFOC control was studied, and the control responses to speed reference changes and to torque were observed. The proposed IFOC algorithm was implemented and tested. In comparison with the DFOC, in the IFOC control, no sensors or modifications are required in the motor, since the rotor flux and speed are estimated based on the mathematical model and measurements of the motor currents. The experimental results demonstrated the efficiency and feasibility of the proposed IFOC algorithm.

REFERENCES

1. Casadei D, Serra G, Tani A, Zarri L (2013). Direct torque control for induction machines: a technology status review. 2013 IEEE Workshop on Conference Electrical Machines Design Control and Diagnosis (WEMDCD). pp. 117–129.
2. Guo Z, Zhang J, Sun Z, Zheng C (2017). Indirect field-oriented control of three-phase induction motor based on current-source inverter. 13th Global Congress on Manufacturing and Management. Procedia Engineering 174 (2017)588-594.
3. Holzmuller T. (2017) Compensation of Delay Time in the Current Control Loop of Field-Oriented Control. In: 19th European Conference on Power Electronics and Applications, p. 1-8.
4. Horvath K.; Kuslits M. (2017) Speed Sensorless Field Oriented Control of Induction Machines Using Unscented Kalman Filter. In: 2017 International Conference on Optimization of Electrical and Electronic Equipment & 2017 INTL Aegean Conference on Electrical Machines and Power Electronics, p. 523-528.
5. Ibrahim S O, Faris K N, Elzahab E A (2015). Implementation of fuzzy modeling system for faults detection and diagnosis in three phase induction motor drive system. Journal of Electrical System and Information Technology. 2:27-46.
6. Leedy A. W. (2013) Simulink/MATLAB Dynamic Induction Motor Model for Use as A Teaching and Research Tool, International Journal of Soft and Engineering, v. 3, n. 4.
7. Leonard W. (2001) Control of Electrical Drives", 3.ed. Nova York: Springer, ISBN 3-540-59380-2.
8. Karimi S, Poure P, Berviller, Y, Saadate S (2007). A design methodology for power electronics digital control based on a FPGA in the loop prototyping. 14th IEEE International Conference on Electronics, Circuits and Systems (ICECS), pp.701-704.
9. Martinez-Hernandez M. A.; Gutierrez-Villalobos J. M.; Malagonsoldara S. M.; Mendoza-Mondragon F.; Rodriguez-Resendiz J. A. (2016) Speed Performance Comparative of Field Oriented Control and Scalar Control for Induction Motors. In: IEEE Conference on Mechatronics, Adaptive and Intelligent Systems, p. 1-7.
10. Matic P, Vukosavic SN (2011). Direct Torque Control of Induction Motor in Field Weakening Without Outer Flux Trajectory Reference. International Review of Electrical Engineering. 7(2):1204-1212.
11. Murphy JMD, Turnbull FG. Power Electronic of AC Motors. Franklin Book Company, ISBN 0080226833. P.524.
12. Niu F, Wang B, Babel AS, Li K, Strangas EG (2016). Comparative Evaluation of Direct Torque Control Strategies for Permanent Magnet Synchronous Machines. Power Electronics, IEEE Transactions on. 31(2):1408-1424.
13. Novotny, D. W and Lipo, T.A. (2000) Vector Control and Dynamics of AC Drives, Oxford Science Publications, ISBN 0-19-856439-2
14. Pandya SN, Chatterjee JK (2010). Torque ripple reduction in direct torque control-based induction motor drive using novel optimal controller design technique. Power Electronics Drives and Energy Systems (PEDES) & 2010 Power India, 2010 Joint International Conference on, pp.1-7.
15. Pereira WCA, Aguiar MI, Paula GT, Monteiro JRBA, Bazan GH, Castoldi MF, Sanches DS (2015). Virtual Platform of direct torque control of induction motor to assist in education of undergraduate students." 2015 IEEE 24th International Symposium on Industrial Electronics (ISIE), pp. 814-818.
16. Perry DL, VHDL Programming by Examples. New York, NY, USA: McGraw-Hill, 2004.
17. Soufien G, Abdellafit M, Mohamed FM (2015). Design and experimental Implementation of DTC of an induction machine based on Fuzzy logic control on FPGA. IEEE Transactions on Fuzzy Systems. 23(3):644-655.
18. Sandre-Hernandez O, Rangel-Magdaleno JJ, Morales-Caporal R (2016). Implementation of direct torque control for a PM synchronous machine based on FPGA. 13th International Conference on Power Electronics (CIEP), pp. 155-160.